AGU PUBLICATIONS

JGR

Journal of Geophysical Research: Oceans

RESEARCH ARTICLE

10.1002/2016JC011715

The Atlantic Water boundary current in the Nansen Basin: Transport and mechanisms of lateral exchange

Kjetil Våge[1], Robert S. Pickart[2], Vladimir Pavlov[3], Peigen Lin[2,4], Daniel J. Torres[2], Randi Ingvaldsen[5], Arild Sundfjord[3], and Andrey Proshutinsky[2]

[1]Geophysical Institute, University of Bergen and Bjerknes Centre for Climate Research, Bergen, Norway, [2]Woods Hole Oceanographic Institution, Woods Hole, Massachusetts, USA, [3]Norwegian Polar Institute, Tromsø, Norway, [4]State Key Laboratory of Marine Environmental Science, College of Ocean and Earth Sciences, Xiamen University, Xiamen, China, [5]Institute of Marine Research, Bergen, Norway

Key Points:
- Data from a shipboard survey are used to investigate the Atlantic Water boundary current north of Svalbard
- The transport of Atlantic Water in the boundary current is quantified
- The roles of eddies and upwelling in lateral exchange between the boundary current and the interior Nansen Basin are examined

Correspondence to:
K. Våge,
kjetil.vage@gfi.uib.no

Citation:
Våge, K., R. S. Pickart, V. Pavlov, P. Lin, D. J. Torres, R. Ingvaldsen, A. Sundfjord, and A. Proshutinsky (2016), The Atlantic Water boundary current in the Nansen Basin: Transport and mechanisms of lateral exchange, *J. Geophys. Res. Oceans*, *121*, 6946–6960, doi:10.1002/2016JC011715.

Received 10 FEB 2016
Accepted 19 AUG 2016
Accepted article online 24 AUG 2016
Published online 22 SEP 2016

Abstract Data from a shipboard hydrographic survey near 30°E in the Nansen Basin of the Arctic Ocean are used to investigate the structure and transport of the Atlantic Water boundary current. Two high-resolution synoptic crossings of the current indicate that it is roughly 30 km wide and weakly middepth-intensified. Using a previously determined definition of Atlantic Water, the transport of this water mass is calculated to be 1.6 ± 0.3 Sv, which is similar to the transport of Atlantic Water in the inner branch of the West Spitsbergen Current. At the time of the survey a small anticyclonic eddy of Atlantic Water was situated just offshore of the boundary current. The data suggest that the feature was recently detached from the boundary current, and, due to compensating effects of temperature and salinity on the thermal wind shear, the maximum swirl speed was situated below the hydrographic property core. Two other similar features were detected within our study domain, suggesting that these eddies are common and represent an effective means of fluxing warm and salty water from the boundary current into the interior. An atmospheric low-pressure system transiting south of our study area resulted in southeasterly winds prior to and during the field measurements. A comparison to hydrographic data from the Pacific Water boundary current in the Canada Basin under similar atmospheric forcing suggests that upwelling was taking place during the survey. This provides a second mechanism related to cross-stream exchange of heat and salt in this region of the Nansen Basin.

1. Introduction

The circulation and modification of Atlantic Water is a fundamental aspect of the Arctic Ocean and plays a critical role in Earth's climate system. This warm intermediate layer was first observed more than 100 years ago by *Nansen* [1902], who concluded that it originated from the North Atlantic Ocean. The Atlantic Water supplies heat and salt to the Arctic Ocean which impacts the thermohaline structure of the water column and likely influences the distribution of sea ice [e.g., *Rudels*, 2012]. Its transformation within the Arctic Ocean provides an important source of water to the deep limb of the global Meridional Overturning Circulation. Indeed, among the constituents of Denmark Strait Overflow Water is Atlantic-origin water that reenters the Nordic Seas within the East Greenland Current after modification in the Arctic Ocean [*Mauritzen*, 1996].

One of the two primary inflows of Atlantic Water into the Arctic Ocean is through the Fram Strait via the West Spitsbergen Current (Figure 1). A portion of the Atlantic Water recirculates and becomes part of the southward flowing East Greenland Current [*Schauer et al*., 2004; *Hattermann et al*., 2016], while the remainder enters the Arctic Ocean. The most recent transport estimate of this northward flow is 3.0 ± 0.2 Sv (1 Sv = 10^6 m^3/s) for water warmer than 2°C, as measured by a long-term moored array across the Fram Strait south of 79°N [*Beszczynska-Möller et al*., 2012]. In the northern part of the strait the inflow splits into two branches (Figure 1). The offshore branch follows the lower part of the continental slope along the western flank of the Yermak Plateau, while the inshore branch flows along the Spitsbergen shelfbreak [e.g., *Aagaard et al*., 1987; *Gascard et al*., 1995].

Farther downstream, a second major inflow of Atlantic Water into the Arctic Ocean occurs through the St. Anna Trough via the Barents Sea [*Schauer et al*., 2002]. This water is markedly colder than the Fram Strait

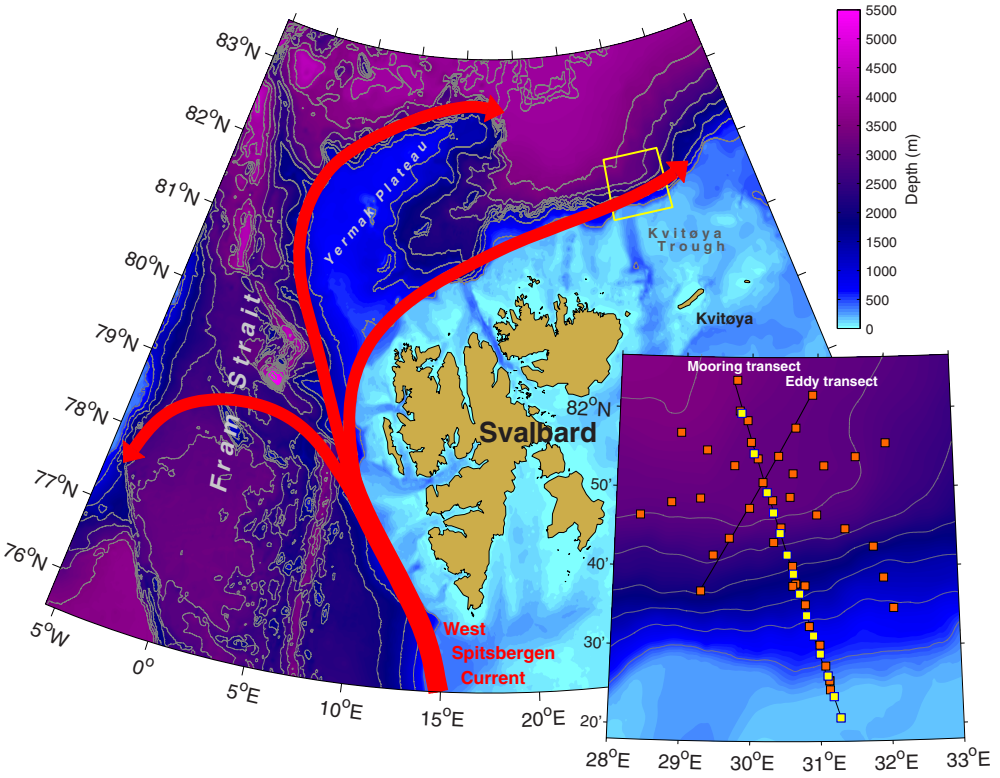

Figure 1. Schematic of the Atlantic Water inflow to the Arctic Ocean through the Fram Strait. The A-TWAIN survey area is indicated by the yellow box and shown in detail in the inset. The mooring and eddy transects are identified. The orange and yellow squares represent locations of shipboard and expendable hydrographic profiles, respectively. Bottom depth is shaded according to the key and contoured with 500 m increments starting at 500 m.

water due to the intense heat loss in the southern Barents Sea [*Smedsrud et al*., 2010]. Rapid transformation of the boundary current properties takes place near the mouth of St. Anna Trough where the two types of Atlantic Water meet. It is presently unclear to what extent the Fram Strait inflow remains part of the boundary current beyond this point; it has recently been argued that this warmer Atlantic Water is mostly diverted into the interior basin in this region [*Rudels*, 2012; *Rudels et al*., 2013] apart from some portion that mixes with the Barents Sea branch of the inflow [*Rudels et al*., 2015].

The remaining Atlantic Water in the boundary current continues to flow cyclonically around the perimeter of the deep Arctic Ocean [*Rudels et al*., 1999]. This pathway was first deduced from the decreasing core temperature of the water along the boundary [e.g., *Coachman and Barnes*, 1963]. Later studies, based on hydrographic surveys and limited current meter data, mapped the boundary current in more detail and argued for the presence of cyclonic gyres in each of the subbasins of the Arctic Ocean [*Aagaard*, 1981; *Rudels et al*., 1994]. A recent high-resolution numerical simulation successfully reproduced the circumpolar boundary current [*Aksenov et al*., 2011], but the model indicated, in contrast to the assertions of *Rudels* [2012] and *Rudels et al*. [2013], that Atlantic Water from the Fram Strait branch is present around the entire Arctic Ocean as opposed to being diverted away from the boundary near St. Anna Trough and confined to the Nansen Basin.

Observational transport estimates of the Atlantic Water boundary current are rare. Based on sparse moored measurements and synoptic hydrographic sections in the area where the Lomonosov Ridge intersects the Eurasian continental slope, *Woodgate et al*. [2001] estimated a boundary current transport of 5 ± 1 Sv approaching the ridge. From current meter records along and beyond the ridge they concluded that the transport was evenly divided between flow along the ridge and a continuation of the boundary current along the slope, consistent with the schematic circulation pattern of *Rudels et al*. [1994]. It has recently been documented that the speed of the current decreases downstream from the Fram Strait and that the current undergoes a structural transformation. Specifically, the current changes from largely barotropic in the Fram

Strait, to middepth-intensified along the Nansen Basin slope, reverting to predominantly barotropic near the junction between the slope and the Lomonosov Ridge [*Pnyushkov et al*., 2013, 2015].

The underlying reasons why Atlantic Water flows into the Arctic Ocean have been investigated using theoretical considerations and numerical simulations. The flux of potential vorticity associated with the transport and hydrographic structure of the Atlantic Water entering and leaving the Arctic Ocean may be central to the formation of the cyclonic boundary current system [*Yang*, 2005; *Karcher et al*., 2007; *Aksenov et al*., 2011]. *Spall* [2013] argues that the salinity contrast between the Atlantic Water and freshwater coming off the Arctic shelves is ultimately responsible for establishing a lateral gradient in the depth of the halocline and, through thermal wind, is related to the transport of the Atlantic Water boundary current.

Since the warm and salty Atlantic Water layer is present throughout the different basins of the Arctic Ocean, it must readily be fluxed offshore from the boundary current [e.g., *Swift et al*., 1997]. However, high-resolution observations of the Atlantic Water boundary current are lacking, and, consequently, the mechanisms of such lateral exchange remain largely unknown. Results from a tightly spaced moored array across the Pacific Water boundary current in the Canada Basin provide some indication of what processes may be at work downstream of the Fram Strait that flux Atlantic Water from the boundary into the interior. The Pacific Water boundary current is baroclinically and, at times, also barotropically unstable [*Spall et al*., 2008; *von Appen and Pickart*, 2012] and is a source of eddies that are known to populate the interior Canada Basin [e.g., *Manley and Hunkins*, 1985; *Kadko et al*., 2008; *Zhao et al*., 2014]. Shipboard hydrographic surveys in the Eurasian Basin suggest that the Atlantic Water boundary current may be similarly unstable [*Schauer et al*., 1997], which is supported by observations of isolated mesoscale features that appear to be Atlantic Water eddies [*Cokelet et al*., 2008; *Zhao et al*., 2014].

Winds along the Eurasian slope likely provide another mechanism to divert Atlantic Water from the boundary into the interior and have been shown to influence the cross-shelf exchange of waters west and north of Svalbard [*Cottier et al*., 2007; *Lind and Ingvaldsen*, 2012]. This exchange process is also at work in the Pacific Water boundary current [*Nikolopoulos et al*., 2009], where easterly winds along the north slope of Alaska periodically reverse the flow and cause upwelling of subsurface waters, which leads to an offshore transport of the Pacific Water [*Pickart et al*., 2009]. This process takes place even in the presence of complete sea ice cover [as long as the ice is mobile, *Schulze and Pickart*, 2012].

The area north of Svalbard, immediately downstream of the Fram Strait, is subject to high heat loss to the atmosphere which leads to substantial modification of the Atlantic Water [*Aagaard et al*., 1987; *Cokelet et al*., 2008]. The pronounced decline of sea ice extent in the Arctic Ocean over the past two decades [e.g., *Comiso*, 2012] has also been documented in this region, attributed in part to increasing temperatures of the Atlantic Water [*Onarheim et al*., 2014]. However, to date there have been no robust transport estimates of the Atlantic Water boundary current downstream of Fram Strait.

In this study we use data from a hydrographic/velocity survey carried out in September 2012 north of Svalbard near 30°E across the shelfbreak and continental slope. The primary purpose of the cruise was to deploy a mooring array across the Atlantic Water boundary current (the results of which will be presented separately). In addition to the mooring operations, a set of shipboard sections was occupied primarily downstream and offshore of the Kvitøya Trough (Figure 1). Using these data, our main objective is to obtain a robust (synoptic) transport estimate of the Atlantic Water boundary current north of Svalbard, examine the structure of the flow, and shed light on aspects of the lateral exchange processes that flux water to and from the boundary current. The data set and methods are presented in section 2. The structure and transport of the boundary current are investigated and quantified in section 3. During the survey an Atlantic Water eddy was observed offshore of the boundary current; this is described in section 4. Finally, in section 5 we consider the effect of wind forcing on the boundary current system, in particular the response of the current to easterly winds that preceded the hydrographic survey.

2. Data and Methods

The "Long-term variability and trends in the Atlantic Water inflow region" (A-TWAIN) project is an international effort to investigate and monitor the Atlantic Water boundary current downstream of Fram Strait using moorings and hydrographic surveys. The program was initiated in September 2012 with the deployment of

eight moorings near 30°E across the continental slope north of Svalbard, and one mooring roughly 150 km upstream of this. A hydrographic/velocity survey conducted during the deployment cruise aboard the R/V *Lance* is the subject of this study (Figure 1). Prior to the mooring deployments the bathymetry along the main mooring line was mapped using the ship's echo sounder, while dropping expendable conductivity-temperature-depth (CTD) probes. The profile data were used to sound-speed correct the bottom data and also served as a hydrographic transect across the boundary current. The full shipboard survey consisted of six near-synoptic sections (Figure 1, inset). Three of these were obtained along the mooring line, while the remaining three sections sampled an Atlantic Water eddy near the base of the continental slope. Apart from the first section along the mooring transect, the hydrographic measurements were obtained using a Sea-Bird CTD instrument. The conductivity sensor was calibrated against in situ salinity samples from the bottom of each cast, and the accuracies of the pressure, temperature, and salinity measurements are estimated to be 0.3 db, 0.001°C, and 0.002, respectively. For the expendable CTD data the accuracies are taken to be 1 m, 0.02°C, and 0.04 in depth, temperature, and salinity, respectively [*Kadko et al*., 2008]. Velocities were measured using a vessel-mounted acoustic Doppler current profiler (ADCP). The Arctic Ocean 5 km tidal model [*Padman and Erofeeva*, 2004] was used to remove the barotropic tidal component from the processed ADCP velocity profiles.

Vertical sections of potential temperature, salinity, potential density, and ADCP velocity were constructed using Laplacian-spline interpolation with a grid spacing of $\Delta x = 2$ km in the horizontal and $\Delta z = 10$ m in the vertical. Using the gridded temperature and salinity fields, the relative geostrophic velocity normal to each section was calculated. Absolute geostrophic velocities were then computed by referencing the relative geostrophic velocity field to the vertically averaged ADCP velocities over the depth interval 30–130 m at each horizontal grid point. Lateral maps of hydrographic properties were made by interpolating the data onto a regular 0.2° longitude by 0.025° latitude grid. We used an algorithm that increases the effective radius along isobaths in regions of steep bathymetry and hence takes into account the greater correlation length scales along bottom topography (see *Våge et al*. [2013] for details of this procedure). This is appropriate given the close alignment between the circulation in the Arctic Ocean and the bottom contours [e.g., *Nøst and Isachsen*, 2003]. Bathymetry data were obtained from the International Bathymetric Chart of the Arctic Ocean (IBCAO) version 3.0 [*Jakobsson et al*., 2012] and smoothed by convolution with a 5 km Gaussian window. The IBCAO bathymetry was in reasonable agreement with the measured bottom depths along the mooring transect, with a root mean square difference of about 10%.

Errors associated with the absolutely-referenced geostrophic velocities were estimated following *Våge et al*. [2011]. The ADCP instrument error (±2 cm/s) and inaccurate bathymetry in the tidal model (±3 cm/s) were the primary sources of uncertainty. The instrument error was lower than that estimated by *Våge et al*. [2011], likely due to averaging over a longer sampling interval. Errors resulting from flow through the "bottom triangles," i.e., the area below the deepest common level of neighboring hydrographic stations, were negligible. The total uncertainty was determined as the root of the sum of the squares of the instrument and tidal model errors. For the transport calculations it was assumed that the error was uncorrelated across the section.

Atmospheric data used in the study were obtained from the global Interim Reanalysis (ERA-I) of the European Center for Medium Range Weather Forecasts [*Dee et al*., 2011]. We use the 6 hourly fields for the month of September 2012, which have a spatial resolution of 0.75°.

3. The Atlantic Water Boundary Current

3.1. Structure

The mooring transect extends from the outer continental shelf north of the island Kvitøya in the Svalbard archipelago into the Nansen Basin of the Arctic Ocean (Figure 1). The transect protrudes sufficiently far into the interior to capture the full transport of Atlantic Water from the inshore branch of the Fram Strait inflow. The fate of the Atlantic Water transported by the offshore branch flowing around the Yermak Plateau is presently unknown, although it is likely that a portion of that Atlantic Water joins the inshore branch upstream of the mooring transect and is thus included in our estimate.

The mean hydrographic profiles from the survey illustrate the hydrographic structure of the water column (Figure 2). The warm and saline Atlantic layer is found between approximately 100 and 500 m; its

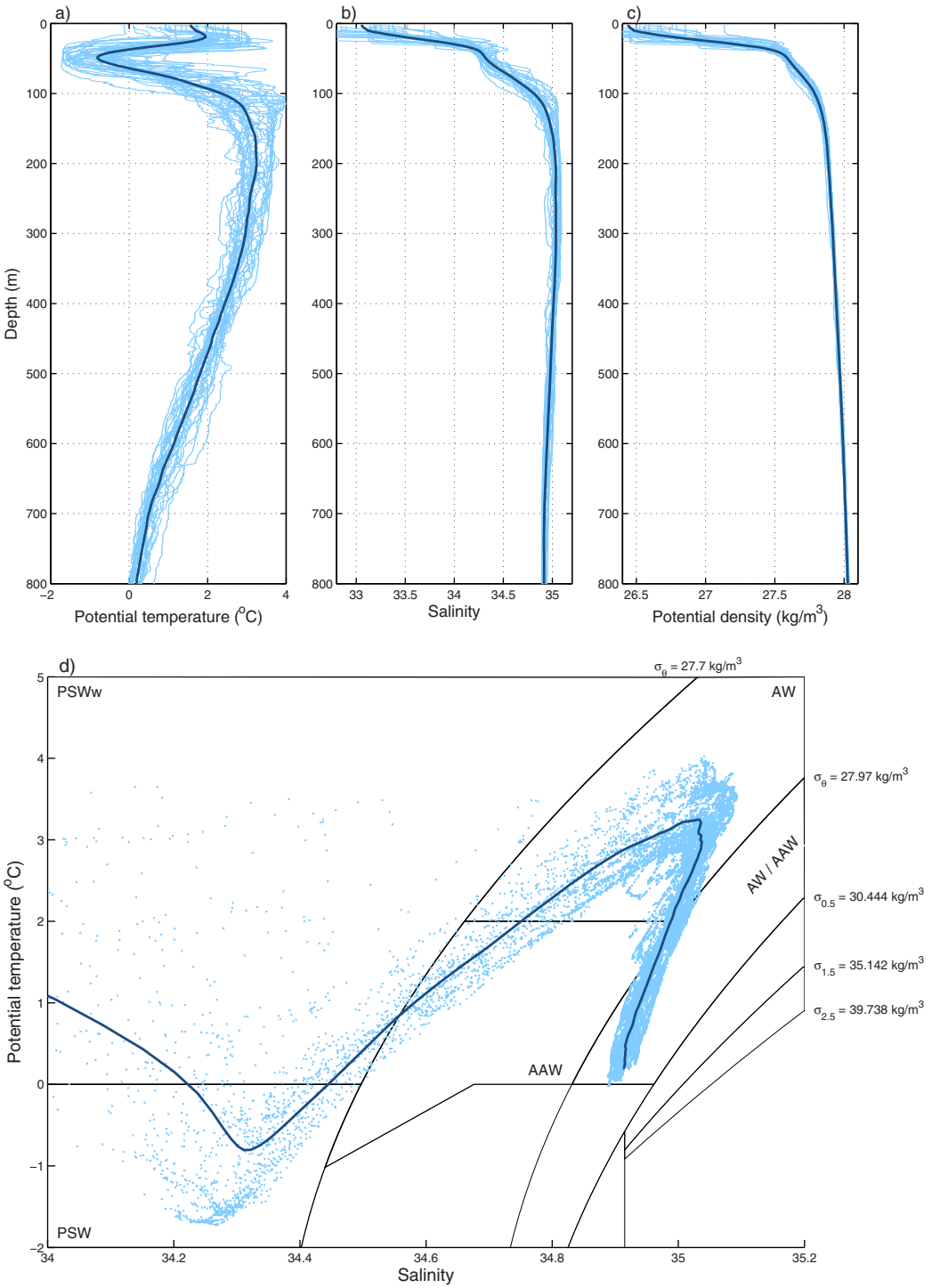

Figure 2. Profiles of (a) potential temperature (θ), (b) salinity (S), (c) potential density, and (d) θ-S curves from the upper 800 m of the survey. Only profiles deeper than 250 m are included. The thin blue lines/dots are individual profiles, while the thick blue line is the mean. The water mass definitions are those from *Rudels et al.* [2005]. The acronyms are: PSW = Polar Surface Water; PSWw = warm Polar Surface Water; AW = Atlantic Water; AAW = Arctic Atlantic Water.

intermediate-depth maximum in temperature and salinity is clearly evident in Figure 2d. A layer of cold, fresh Polar Surface Water, which also includes the halocline, resides above the Atlantic Water [*Rudels et al.*, 2005]. Below the Atlantic layer are colder intermediate waters and the deep waters of the Arctic Ocean. This

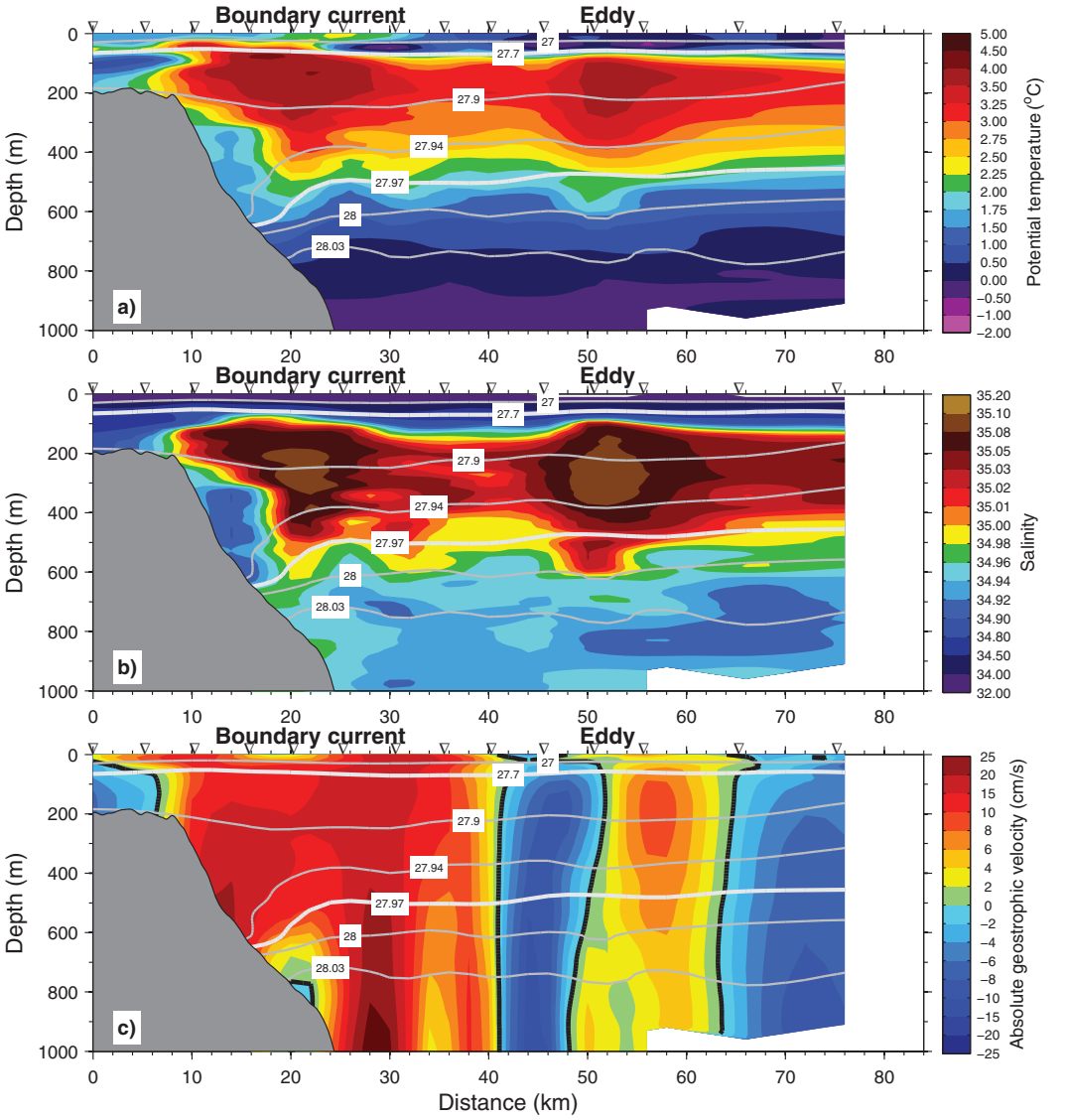

Figure 3. Vertical sections of (a) potential temperature, (b) salinity, and (c) absolute geostrophic velocity (positive values indicate northeastward flow) along the mooring transect marked in Figure 1. The expendable CTD section was occupied over 6 h on 16 September 2012. The gray lines are contours of potential density (the 27.70 and 27.97 kg/m^3 isopycnals, taken to be the density limits of the Atlantic Water, are highlighted). The inverted triangles indicate the station locations, and the locations of the boundary current and the core of the Atlantic Water eddy are marked.

hydrographic structure is similar to that of previous hydrographic sections occupied in the vicinity of the mooring transect [*Schauer*, 1995; *Schauer et al*., 1997; *Cokelet et al*., 2008; *Ivanov et al*., 2009].

Two occupations of the inner part of the mooring line were separated by only a few hours and they are similar in character; hence, only the first section is considered here. An extremum in temperature and salinity within the Atlantic layer was situated above the upper part of the continental slope, offshore of the shelfbreak (Figures 3a and 3b). The absolute geostrophic velocity reveals that this water constituted the core of the Atlantic Water boundary current (Figure 3c). The current was roughly 30 km wide (x = 10–40 km), and, inshore of x = 25 km, it was weakly middepth-intensified. (We note that the bottom-intensified flow near x = 30 km was not present on the second occupation and is deeper than the Atlantic Water layer.) This is consistent with the structure of the boundary current from Fram Strait to the Svalbard slope described by *Pnyushkov et al*. [2013]. The strength of the boundary current within the Atlantic Water layer was 15–20 cm/s. Interestingly, a small amount of cold, fresh water on the upper slope near x = 14 km was present in both of

Table 1. Definitions of Atlantic Water and Corresponding Transport Estimates

Transport of Atlantic Water (Sv)	Definition of Atlantic Water
1.6 ± 0.3	$27.70 \leq \sigma_\theta \leq 27.97$ kg/m^3 and $\theta \geq 2$°C
1.8 ± 0.3	$27.70 \leq \sigma_\theta \leq 27.97$ kg/m^3 and $\theta \geq 1$°C
2.5 ± 0.6	$\sigma_\theta \geq 27.70$ kg/m^3 and $\sigma_{0.5} \leq 30.444$ kg/m^3 and $\theta \geq 0$°C

the synoptic occupations. This is likely a remnant of deeper water that was previously upwelled, and is discussed further in section 5.

Farther offshore, near x = 50 km, a second maximum in temperature and salinity was present in all three occupations of the mooring line (Figure 3). This was the core of an Atlantic Water eddy, presumably spun off the boundary current sometime in the past. The absolute geostrophic velocity field demonstrates that the eddy was rotating anticyclonically. This feature is investigated in more detail in section 4.

3.2. Transport

Although the second occupation of the mooring line did not extend as far offshore as the first, it was sufficiently long to span the boundary current. Both of these were synoptic crossings, taking 6 and 48 h, respectively, to complete. During the deployment of the moorings a third occupation was done as well, but this covered only the outer part of the transect and did not sample the boundary current. The volume flux of Atlantic Water was computed by integrating the eastward flow from the inshore end of the section to the location of the eddy. Following *Rudels et al*. [2005] we considered Atlantic Water to be within the density range $27.70 \leq \sigma_\theta \leq 27.97$ kg/m^3 and warmer than 2°C. The corresponding transport of Atlantic Water across the first section was 1.7 ± 0.5 Sv, while that for the second section was 1.5 ± 0.4 Sv. As noted above, the two sections were taken only hours apart, and it is presently unknown what the decorrelation time scale of the boundary current is. If these can be considered as independent realizations, then the mean volume flux of Atlantic Water in the boundary current north of Svalbard was 1.6 ± 0.3 Sv during the period of the survey. Relaxing the temperature criterion to 1°C [but retaining the density limits, e.g., *Schauer et al*., 2004] resulted in an increase of the mean transport to 1.8 ± 0.3 Sv. Expanding the definition even further to include Atlantic-origin intermediate waters (AW and AAW in Figure 2d), and hence the bulk of the upper 1000 m of the boundary current, resulted in a mean transport of 2.5 ± 0.6 Sv (the details of these transport calculations are shown in Table 1).

How do these values compare to the measurements at Fram Strait? Using nearly the same restrictive definition of Atlantic Water, *Beszczynska-Möller et al*. [2012] estimated a transport of 3.0 ± 0.2 Sv. Of this, 1.3 ± 0.1 Sv was associated with the core of the West Spitsbergen Current, i.e., the inshore branch of the Fram Strait inflow, while the remaining 1.7 ± 0.1 Sv formed the offshore branch along the Yermak Plateau. Bearing in mind that our estimate is a synoptic value in contrast to the Fram Strait estimate, which is based on a long-term time series, and that the Atlantic Water flow exhibits substantial variability on seasonal and shorter time scales [*Beszczynska-Möller et al*., 2012; *Randelhoff et al*., 2015], it does nonetheless suggest that the boundary current near 30°E is predominantly the downstream extension of the inshore branch of the West Spitsbergen Current, with perhaps a contribution from the Atlantic Water that flows around the Yermak Plateau. This is in accordance with recent high-resolution numerical simulations of the Atlantic Water inflow through Fram Strait in which a portion of the offshore branch rejoins the inner branch downstream of the Yermak Plateau [*Kawasaki and Hasumi*, 2015]. However, the proportion of the Atlantic Water which progresses from the Fram Strait into the boundary current north of Svalbard in that model (about one third) is less than our synoptic estimate.

4. An Atlantic Water Eddy

As noted above, a rotating lens of Atlantic Water offshore of the boundary current was observed near x = 50 km along the mooring transect (Figure 3). The eddy remained largely stationary during the week that R/V *Lance* was in the area, and it was sampled by multiple hydrographic/velocity sections. This allowed us to construct a lateral map of the feature. Figure 4 shows the mean salinity of the Atlantic Water layer overlaid by the absolute geostrophic velocity vectors (realizing that these are not true vectors since they only depict the flow normal to each transect). This reveals that the core of the eddy was roughly circular, with a diameter of 20–30 km, and it was rotating anticyclonically. The map of potential temperature (not shown) displays analogous features.

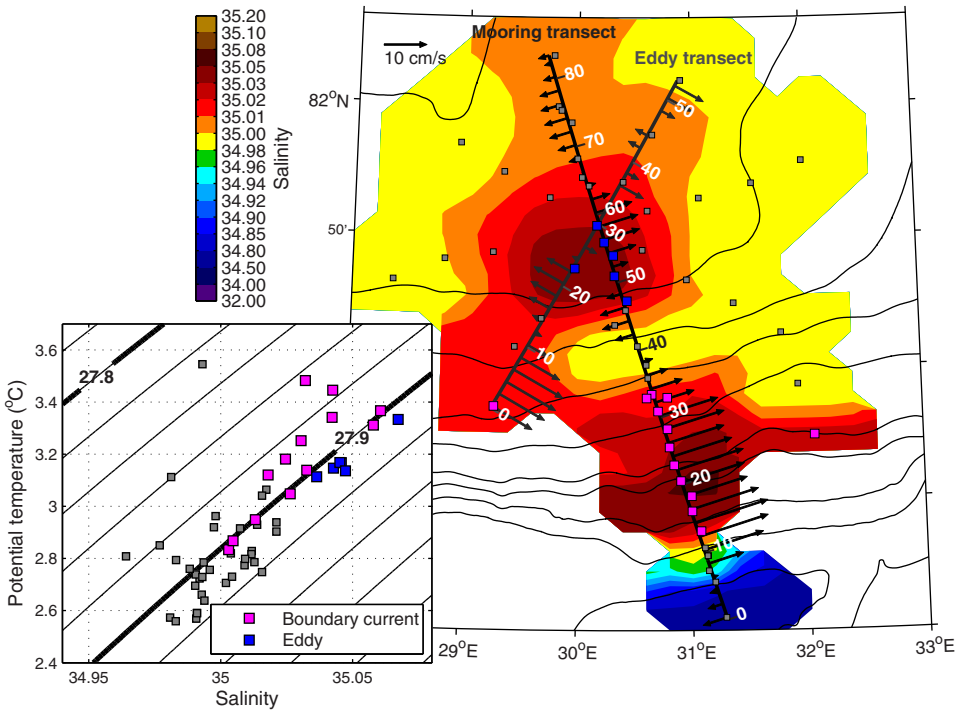

Figure 4. Lateral map of salinity (color) and absolute geostrophic velocity (vectors) from the mooring and eddy transects averaged over the Atlantic Water layer ($27.70 \leq \sigma_\theta \leq 27.97$ kg/m^3 and $\theta \geq 2$°C, see text). The location of each station is indicated by a square. Stations within the boundary current and the eddy are marked by magenta and blue colors, respectively, while the remaining stations are colored gray. The numbers indicate distance (in km) along the mooring and eddy transects. Every 200 m isobath to 1000 m then every 500 m isobath is contoured. The inset shows the averaged θ-S value for each station.

The southern ends of the transects in Figure 4 sampled the boundary current, indicating that the translational speeds in the eddy were smaller than the advective speeds of the boundary current. While there was a clear separation between the eddy and boundary current on the mooring transect, farther to the west the feature abutted the current, suggesting that it recently spawned from the current or was interacting with it. Figure 4 (inset) shows quantitatively that the core of the eddy was warmer and more saline than the ambient Atlantic Water in the interior; the hydrographic properties of the eddy were similar to the majority of stations within the boundary current. This is also suggestive of a recent boundary current origin. (The few boundary current stations with relatively low potential temperature and salinity were either located near the outskirts of the current or associated with intrusions of colder, fresher water into the current.)

As seen in the lateral map, one of the transects bisected the core of the eddy (called the Eddy transect in Figure 4) and provides the best depiction of the vertical structure of the feature (Figure 5). The property core (elevated temperature and salinity) is centered at approximately 250 m depth. To a large degree the temperature and salinity compensate each other, so that the density signature is more subtle. However, there is a slight doming of the isopycnals in the depth range of roughly 250–500 m, indicating that the salty core of the eddy influences its density more than the temperature (Figure 5a). Below this depth there is a bowling of the isopycnals to roughly 700 m depth as the warm temperatures dominate over the salinity in dictating the density (Figure 5b). The associated thermal wind signature means that the strongest azimuthal speed of the eddy is roughly 250 m deeper than the property core (500 versus 250 m depth, Figure 5c). Furthermore, the velocity signature extends deep into the water column (deeper than 1000 m). Such a deep-reaching swirl speed is consistent with the response of the water column to the injection of a low potential vorticity anomaly (i.e., the Atlantic Water lens) from the boundary current [see *Spall*, 1995].

Pacific Water eddies are commonly observed in the Canada Basin of the Arctic Ocean offshore of the boundary current along the edge of the Chukchi and Beaufort Seas [*Manley and Hunkins*, 1985; *Zhao et al.*, 2014]. These are also middepth-intensified anticyclones, most commonly with a cold core (due to cold Pacific Winter Water), and result from baroclinic instabilities of the boundary current [*Pickart et al.*, 2005; *Spall*

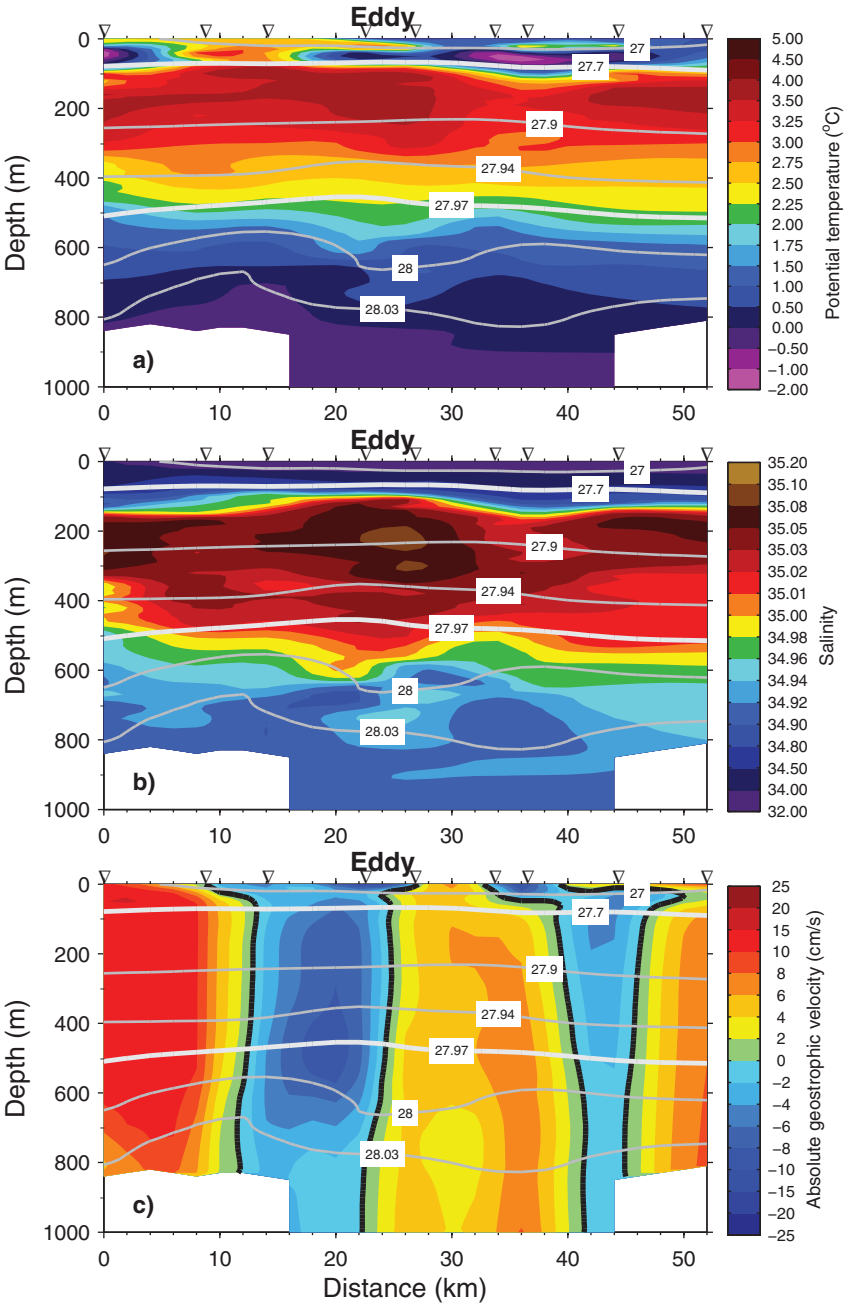

Figure 5. Vertical sections of (a) potential temperature, (b), salinity, and (c) absolute geostrophic velocity along the eddy transect indicated in Figure 4. The section took 35 h to complete between 20 and 22 September 2012. The gray lines are contours of potential density (in kg/m^3), the inverted triangles indicate the station locations, and the position of the core of the Atlantic Water eddy is marked.

et al., 2008]. One fundamental difference between the Pacific Water eddies and the feature observed here is that, in the Canada Basin, the salinity dictates the density (at these cold temperatures). Hence, the temperature core does not dynamically influence the feature, and, as such, the swirl speed of the eddy is strongest at the property core (not displaced vertically as is the case in Figure 5c). Nonetheless, the velocity signature of the Pacific Water eddies also extends far deeper than the property core (R. Pickart, unpublished data).

While the population of Pacific Water eddies in the Canada Basin is quite substantial [*Zhao et al*., 2014] and they have been observed spawning from the boundary current [*Pickart et al*., 2005], it is unknown how prevalent this type of Atlantic Water eddy is in the Eurasian Arctic. However, three such features were observed during our 9-day survey, which suggests that they may be common also in this part of the Nansen Basin. A

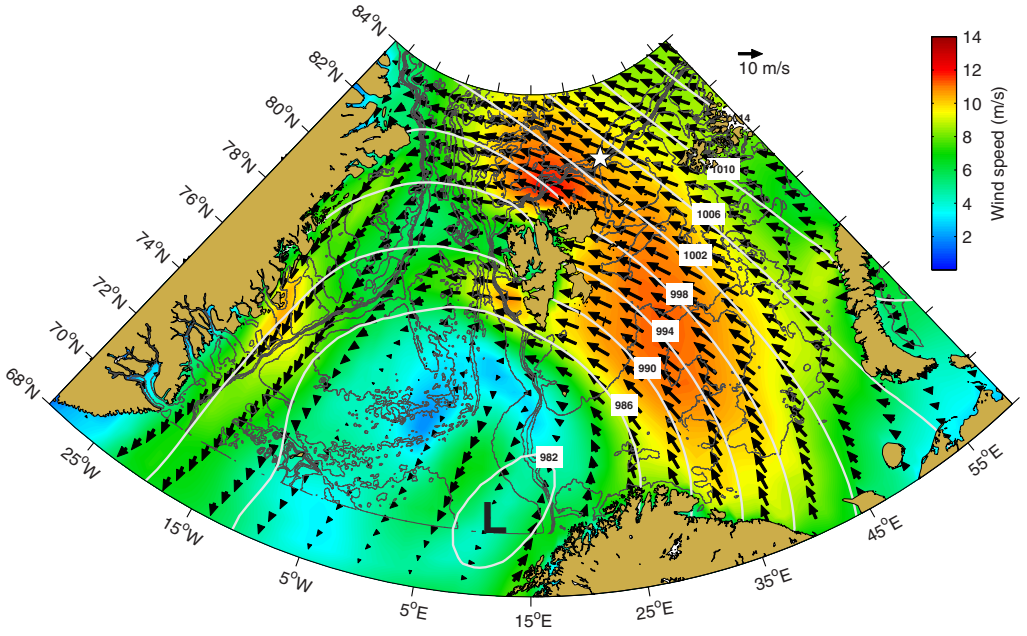

Figure 6. Mean atmospheric conditions on 14–15 September 2012. The sea level pressure (contours, mb) and 10 m winds (color and vectors, m/s) are shown. The mooring transect is marked by the white star. Bathymetry is contoured in 250 m increments from the surface to 1000 m, thereafter in 1000 m increments.

second (weaker) eddy is evident at the offshore end of the eddy transect; note the warm and salty core at the two seaward-most stations in Figure 5 and the anticyclonic rotation associated with the feature (this is seen in the lateral map as well, Figure 4). Furthermore, a similar eddy was measured on the hydrographic transect extending along the 3000 m isobath to the west of the mooring line (not shown). In light of the pronounced layer of Atlantic Water extending far into the basin (Figure 3), it is evident that the lateral flux of this water from the boundary current is substantial. Eddy formation from the boundary current may be among the primary mechanisms of exchange. Fortunately, the mooring array extended sufficiently far offshore to have captured the eddy shown in Figures 4 and 5; hence, the mooring time series will shed more light on this issue.

5. Response to Wind Forcing

Another potential mechanism of exchange between the boundary current and the interior is wind-driven upwelling and downwelling. Our study region is in the vicinity of the North Atlantic storm track [*Wernli and Schwierz*, 2006], and a low-pressure system that transited the Nordic Seas prior to and during the survey resulted in upwelling-favorable conditions. In particular, in the 2–3 days before the first occupation of the mooring line on 16 September, the low was located northwest of northern Norway (Figure 6). The cyclonic circulation around the low resulted in persistent southeasterly winds north of Spitsbergen. Following this, the low-pressure system transited eastward into the Barents Sea and then northeastward. Consequently, the boundary current was subject to easterly alongshore winds of 5–10 m/s for more than a week (Figure 7). Was this forcing enough to lead to upwelling? Based on what is known about upwelling in the Pacific Water boundary current in the Canada Basin, this appears to be the case.

Alongshore easterly winds exceeding 5 m/s consistently result in upwelling in the Pacific Water boundary current along the continental slope of the Beaufort Sea [*Schulze and Pickart*, 2012]. The typical sequence of events is that, once the winds intensify, the boundary current reverses to the west within a matter of hours and upwelling commences shortly thereafter [on average, about 16 h after the increase in the wind, *Pickart et al*., 2009]. The mean transport of the Pacific Water boundary current [0.13 Sv, *Nikolopoulos*

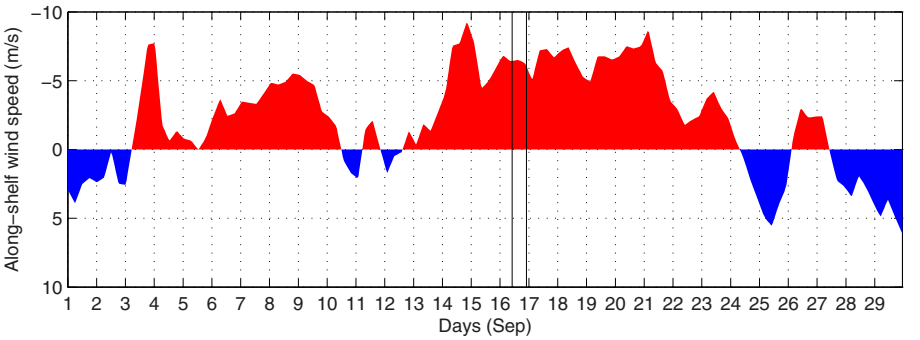

Figure 7. Along-shelf wind near the mooring section during September 2012. Negative values indicate northeasterly (upwelling favorable) winds. The vertical lines mark when the two synoptic crossings of the Atlantic Water boundary current were occupied. Note that the *y* axis is reversed.

et al., 2009] is an order of magnitude smaller than the eastward transport of the Atlantic Water boundary current calculated here; hence, it is unclear if winds of this strength could reverse the Atlantic Water boundary current—it may be that the eastward flow is simply diminished. However, the structure of the density field in Figure 3 is indicative of upwelling, as we will now demonstrate.

An upward deflection of isopycnals onto the shelf was observed during the first shipboard occupation of the mooring line (Figure 8a). This is true for all of the isopycnals less dense than $\sigma_\theta = 27.9$ kg/m^3. Curiously, however, the deeper isopycnals slope downward toward the boundary. In Figure 8a we have calculated the vertical displacement of the isopycnals relative to their depth at the offshore end of the section. One sees a dipole structure onshore, with a positive displacement on the outer shelf/upper slope, and downward displacement deeper on the midslope. Such a signature of diverging isopycnals, upon first glance, seems at odds with the notion of upwelling. However, this exact phenomenon is regularly observed during upwelling conditions on the Beaufort slope.

To demonstrate this, we considered all upwelling events that took place on the Beaufort slope from summer 2002 to summer 2004, during which time there was an array of moorings deployed across the Pacific Water boundary current at 152°W [*Nikolopoulos et al*., 2009]. The events differed in duration, wind forcing, and ice cover. As seen in Table 2, upwelling occurred in each season of the year (a total of 49 events), with the fewest events in summer and the most events in winter. Both the strength of the wind forcing and the duration of the events were similar over the course of the year, with the average values of these quantities comparable to the wind event that occurred north of Svalbard during our field program. Notably, during all of the upwelling events the shallow isopycnals were displaced upward toward the shelfbreak, while the deeper isopycnals were displaced downward.

To quantify this we constructed a composite upwelling event for the 49 storms. Since the central isopycnal where the divergence occurred differed from storm to storm, we adjusted each realization vertically to align this isopycnal. The middle third of the storm is considered most appropriate for comparison with the A-TWAIN section given the timing of the survey relative to the alongshore winds. The resulting composite vertical section of density displacement is shown in Figure 8b, where the vertical displacement of the isopycnals relative to their offshore depth was again computed. The smaller vertical displacement in the Canada Basin is likely due to a stronger stratification, but the same dipole pattern associated with the divergence of isopycnals that was present during the occupation of the A-TWAIN section during enhanced easterly winds is evident. This implies that upwelling was in the process of occurring at the time of the survey and that the isopycnal structure that we observed was not indicative of the normal, unforced boundary current. The cause of the isopycnal divergence is not presently understood, but is likely part of the three-dimensional response of the current to easterly winds. Our results suggest that this response is ubiquitous to both the Pacific and Atlantic Water boundary currents of the Arctic Ocean. Further effort is required to expand upon the relevant dynamics at work and the ramifications for the exchange of mass and properties between the boundary and the interior.

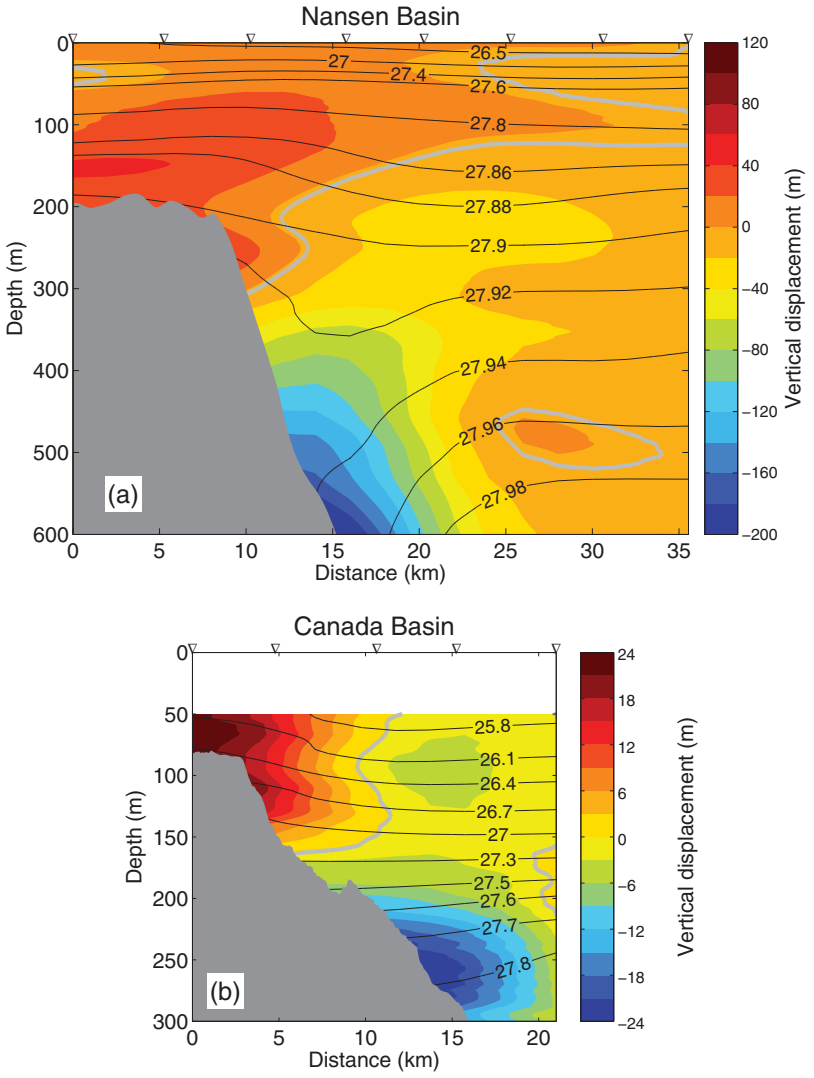

Figure 8. (a) Vertical displacement of isopycnals relative to their depth at the offshore end of the mooring transect and (b) the composite mean of the upwelling events from the Beaufort slope. The inverted triangles indicate (a) station and (b) mooring locations. The gray line is the zero displacement contour.

6. Discussion

From two crossings of the boundary current north of the Svalbard archipelago near 30°E we estimate a transport of Atlantic Water of 1.6 ± 0.3 Sv. Our synoptic estimate is comparable to the 1.3 ± 0.1 Sv transported by the inshore branch of the Fram Strait inflow [*Beszczynska-Möller et al.*, 2012], but likely includes some contribution from the stronger offshore branch which flows along the Yermak Plateau. However, it is important to keep in mind that our estimate is a synoptic value obtained in early fall. The transport of Atlantic Water through Fram Strait is enhanced in winter [*Beszczynska-Möller et al.*, 2012], and the significant

Table 2. Mean Properties of All of the Upwelling Events on the Beaufort Slope Measured by a Mooring Array Deployed From Summer 2002 to Summer 2004

Season	Number of Events	Mean Along-shelf Wind Speed (m/s)	Mean Ice Concentration (%)	Mean Duration (days)
Spring (Mar–May)	11	4.8 ± 0.1	87 ± 1	8.6 ± 2.4
Summer (Jun–Aug)	4	5.3 ± 0.1	36 ± 8	7.6 ± 2.0
Fall (Sep–Nov)	15	5.2 ± 0.1	34 ± 5	4.8 ± 0.9
Winter (Dec–Feb)	19	5.1 ± 0.1	88 ± 1	6.3 ± 1.1

seasonal variability of its hydrographic properties is not eroded between the Fram Strait and the mooring section [*Ivanov et al*., 2009]. It should also be noted that the transport of Atlantic Water may have been diminished during the survey period due to the upwelling-favorable conditions.

The presence of Atlantic Water in the Arctic Ocean is not restricted to the boundary current system; it is found throughout the interior basins at intermediate depths. Hence, processes must be active that efficiently flux Atlantic Water from the boundary into the interior. We have shed light on two likely mechanisms of lateral exchange: eddy transport and wind-driven upwelling. The Pacific Water boundary current in the Canada Basin spawns eddies as a result of barotropic and baroclinic instabilities [*Spall et al*., 2008; *von Appen and Pickart*, 2012]. Shipboard hydrographic surveys in the Eurasian Basin suggest that the Atlantic Water boundary current may be similarly unstable [*Schauer et al*., 1997]. We observed an anticyclonic eddy with a core of Atlantic Water that was warmer and more saline than the ambient water in the interior. The feature was located about 50 km offshore of the shelfbreak near the mooring section. Signatures of two additional Atlantic Water eddies in our study area suggest, in accordance with previous observations of mesoscale disturbances in this region [*Cokelet et al*., 2008], that such features are not uncommon in the Nansen Basin. Similar eddies have previously been observed as well in the northern Fram Strait [e.g., *Gascard et al*., 1995], perhaps resulting from instabilities in the West Spitsbergen Current [*Teigen et al*., 2010, 2011; *von Appen et al*., 2016]. By contrast, *Ivanov et al*. [2009] reported a highly persistent direction of flow from a single mooring deployed within the boundary current in the vicinity of the mooring section and concluded that the Atlantic Water boundary current did not undergo intensive eddy formation in this region. The cross-stream array of moorings deployed during our survey will inform us further on this issue.

Wind-driven upwelling/downwelling may be another mechanism for diverting Atlantic Water from the boundary current into the interior. The magnitude of the easterly winds prior to and during our survey would have been of sufficient strength to drive upwelling in the Pacific Water boundary current in the Canada Basin [*Schulze and Pickart*, 2012]. The vertical displacement of isopycnals observed on the continental slope north of Svalbard during the wind event was consistent with a composite of 49 upwelling events that took place on the Beaufort slope between summer 2002 and summer 2004. This strongly suggests that upwelling was ongoing during the time of the survey.

Our hydrographic/velocity survey downstream of Fram Strait near the Kvitøya Trough indicates that the boundary current is highly dynamic at this location, which results in the injection of Atlantic Water into the interior. This would help maintain the warm and saline intermediate layer that strongly impacts the thermohaline structure of the Arctic Ocean. The moored array deployed at this location will result in a more robust transport estimate and shed light on the mechanisms of cross-stream exchange in this important region, where increasing temperatures of the Atlantic Water may in part be responsible for an accelerating loss of sea ice [*Onarheim et al*., 2014].

Acknowledgments

We thank Wilken-Jon von Appen and two anonymous reviewers for helpful comments on the manuscript. The data used in this study were collected through the project "Long-term variability and trends in the Atlantic Water inflow region" (A-TWAIN). The Norwegian component was funded by the Arctic Ocean program at the FRAM-High North Research Centre for Climate and the Environment. The US part was funded by the Steven Grossman Family Foundation and by the National Science Foundation under grant ARC-1264098. KV received support from the Fulbright Foundation. The data used in this study can be obtained from http://atwain.whoi.edu.

References

Aagaard, K. (1981), On the deep circulation in the Arctic Ocean, *Deep Sea Res., Part A*, *28*, 251–268.

Aagaard, K., A. Foldvik, and S. R. Hillman (1987), The West Spitsbergen Current: Disposition and water mass transformation, *J. Geophys. Res.*, *92*, 3778–3784.

Aksenov, Y., V. V. Ivanov, A. J. G. Nurser, S. Bacon, I. V. Polyakov, A. C. Coward, A. C. N. Garabato, and A. Beszczynska-Möller (2011), The Arctic Circumpolar Boundary Current, *J. Geophys. Res.*, *116*, C09017, doi:10.1029/2010JC006637.

Beszczynska-Möller, A., E. Fahrbach, U. Schauer, and E. Hansen (2012), Variability in Atlantic water temperature and transport at the entrance to the Arctic Ocean, 1997-2010, *ICES J. Mar. Sci.*, *69*, 852–863, doi:10.1093/icesjms/fss056.

Coachman, L. K., and C. A. Barnes (1963), The movement of Atlantic water in the Arctic Ocean, *Arctic*, *16*, 8–16.

Cokelet, E. D., N. Tervalon, and J. G. Bellingham (2008), Hydrography of the West Spitsbergen Current, Svalbard Branch: Autumn 2011, *J. Geophys. Res.*, *113*, C01006, doi:10.1029/2007JC004150.

Comiso, J. C. (2012), Large decadal decline of the Arctic multiyear ice cover, *J. Clim.*, *25*, 1176–1193, doi:10.1175/JCLI-D-11-00113.1.

Cottier, F. R., F. Nilsen, M. E. Inall, S. Gerland, V. Tverberg, and H. Svendsen (2007), Wintertime warming of an Arctic shelf in response to large-scale atmospheric circulation, *Geophys. Res. Lett.*, *34*, L10607, doi:10.1029/2007GL029948.

Dee, D. P., et al. (2011), The ERA-Interim reanalysis: Configuration and performance of the data assimilation system, *Q. J. R. Meteorol. Soc.*, *137*, 553–597, doi:10.1002/qj.828.

Gascard, J.-C., C. Richez, and C. Rouault (1995), New insights on large-scale oceanography in Fram Strait: The West Spitsbergen Current, in *Arctic Oceanography: Marginal Ice Zones and Continental Shelves*, edited by W. O. Smith and J. M. Grebmeier, pp. 131–182, AGU, Washington, D. C.

Hattermann, T., P. E. Isachsen, W.-J. von Appen, J. Albretsen, and A. Sundfjord (2016), Eddy-driven recirculation of Atlantic Water in Fram Strait, *Geophys. Res. Lett.*, *43*, 3406–3414, doi:10.1002/2016GL068323.

Ivanov, V. V., I. V. Polyakov, I. A. Dmitrenko, E. Hansen, I. A. Repina, S. A. Kirillov, C. Mauritzen, H. Simmons, and L. A. Timokhov (2009), Seasonal variability in Atlantic Water off Spitsbergen, *Deep Sea Res., Part I*, *56*, 1–14, doi:10.1016/j.dsr.2008.07.013.

Jakobsson, M., et al. (2012), The International Bathymetric Chart of the Arctic Ocean (IBCAO) version 3.0, *Geophys. Res. Lett.*, *39*, L12609, doi:10.1029/2012GL052219.
Kadko, D., R. S. Pickart, and J. Mathis (2008), Age characteristics of a shelf-break eddy in the western Arctic and implications for shelf-basin exchange, *J. Geophys. Res.*, *113*, C02018, doi:10.1029/2007JC004429.
Karcher, M., F. Kauker, R. Gerdes, E. Hunke, and J. Zhang (2007), On the dynamics of Atlantic Water circulation in the Arctic Ocean, *J. Geophys. Res.*, *112*, C04S02, doi:10.1029/2006JC003630.
Kawasaki, T., and H. Hasumi (2015), The inflow of Atlantic water at the Fram Strait and its interannual variability, *J. Geophys. Res. Oceans*, *121*, 502–519, doi:10.1002/2015JC011375.
Lind, S., and R. B. Ingvaldsen (2012), Variability and impacts of Atlantic Water entering the Barents Sea from the north, *Deep Sea Res., Part I*, *62*, 70–88, doi:10.1016/j.dsr.2011.12.007.
Manley, T. O., and K. Hunkins (1985), Mesoscale eddies of the Arctic Ocean, *J. Geophys. Res.*, *90*, 4911–4930.
Mauritzen, C. (1996), Production of dense overflow waters feeding the North Atlantic across the Greenland-Scotland Ridge. Part 1: Evidence for a revised circulation scheme, *Deep Sea Res., Part I*, *43*, 769–806.
Nansen, F. (1902), Oceanography of the North Polar Basin, in *Norwegian North Polar Expedition 1893-96: Scientific Results*, vol. 3, No. 9, 427 pp.
Nikolopoulos, A., R. S. Pickart, P. S. Fratantoni, K. Shimada, D. J. Torres, and E. P. Jones (2009), The western Arctic boundary current at 152°W: Structure, variability, and transport, *Deep Sea Res., Part II*, *56*, 1164–1181, doi:10.1016/j.dsr2.2008.10.014.
Nøst, O. A., and P. E. Isachsen (2003), The large-scale time-mean ocean circulation in the Nordic Seas and Arctic Ocean estimated from simplified dynamics, *J. Mar. Res.*, *61*, 175–210.
Onarheim, I. H., L. H. Smedsrud, R. B. Ingvaldsen, and F. Nilsen (2014), Loss of sea ice during winter north of Svalbard *Tellus, Ser. A*, *66*, 23933, doi:10.3402/tellusa.v66.23933.
Padman, L., and S. Erofeeva (2004), A barotropic inverse tidal model for the Arctic Ocean, *Geophys. Res. Lett.*, *31*, L02303, doi:10.1029/2003GL019003.
Pickart, R. S., T. J. Weingartner, L. J. Pratt, S. Zimmermann, and D. J. Torres (2005), Flow of winter-transformed Pacific Water into the western Arctic, *Deep Sea Res., Part II*, *52*, 3175–3198.
Pickart, R. S., G. W. K. Moore, D. J. Torres, P. S. Fratantoni, R. A. Goldsmith, and J. Yang (2009), Upwelling on the continental slope of the Alaskan Beaufort Sea: Storms, ice, and oceanographic response, *J. Geophys. Res.*, *114*, C00A13, doi:10.1029/2008JC005009.
Pnyushkov, A. V., I. V. Polyakov, V. V. Ivanov, and T. Kikuchi (2013), Structure of the Fram Strait branch of the boundary current in the Eurasian Basin of the Arctic Ocean, *Polar Sci.*, *7*, 53–71, doi:10.1016/j.polar.2013.02.001.
Pnyushkov, A. V., I. V. Polyakov, V. V. Ivanov, Y. Aksenov, A. C. Coward, M. Janout, and B. Rabe (2015), Structure and variability of the boundary current in the Eurasian Basin of the Arctic Ocean, *Deep Sea Res., Part I*, *101*, 80–97, doi:10.1016/j.dsr.2015.03.001.
Randelhoff, A., A. Sundfjord, and M. Reigstad (2015), Seasonal variability and fluxes of nitrate in the surface waters over the Arctic shelf slope, *Geophys. Res. Lett.*, *42*, 3442–3449, doi:10.1002/2015GL063655.
Rudels, B. (2012), Arctic Ocean circulation and variability—Advection and external forcing encounter constraints and local processes, *Ocean Sci.*, *8*, 261–286, doi:10.5194/os-8-261-2012.
Rudels, B., E. P. Jones, L. G. Anderson, and G. Kattner (1994), On the intermediate depth waters of the Arctic Ocean, in *The Polar Oceans and Their Role in Shaping the Global Environment*, edited by O. M. Johannesen, R. D. Muench, and J. E. Overland, pp. 33–46, AGU, Washington, D. C.
Rudels, B., H. J. Friedrich, and D. Quadfasel (1999), The Arctic circumpolar boundary current, *Deep Sea Res., Part II*, *46*, 1023–1062.
Rudels, B., G. Björk, J. Nilsson, P. Winsor, I. Lake, and C. Nohr (2005), The interaction between waters from the Arctic Ocean and the Nordic Seas north of Fram Strait and along the East Greenland Current: Results from the Arctic Ocean-02 Oden expedition, *J. Mar. Syst.*, *55*, 1–30.
Rudels, B., U. Schauer, G. Björk, M. Korhonen, S. Pisarev, B. Rabe, and A. Wisotzki (2013), Observations of water masses and circulation with focus on the Eurasian Basin of the Arctic Ocean from the 1990s to the late 2000s, *Ocean Sci.*, *9*, 147–169, doi:10.5194/os-9-147-2013.
Rudels, B., M. Korhonen, U. Schauer, S. Pisarev, B. Rabe, and A. Wisotzki (2015), Circulation and transformation of Atlantic water in the Eurasian Basin and the contribution of the Fram Strait inflow branch to the Arctic Ocean heat budget, *Prog. Oceanogr.*, *132*, 128–152, doi:10.1016/j.pocean.2014.04.003.
Schauer, U. (1995), The release of brine-enriched shelf water from Storfjord into the Norwegian Sea, *J. Geophys. Res.*, *100*, 16,015–16,028.
Schauer, U., R. D. Muench, B. Rudels, and L. Timokhov (1997), Impact of eastern Arctic shelf waters on the Nansen Basin intermediate layers, *J. Geophys. Res.*, *102*, 3371–3382.
Schauer, U., H. Loeng, B. Rudels, V. K. Ozhigin, and W. Dieck (2002), Atlantic Water flow through the Barents and Kara seas, *Deep Sea Res., Part I*, *49*, 2281–2298, doi:10.1029/2003JC001823.
Schauer, U., E. Fahrbach, S. Østerhus, and G. Rohardt (2004), Arctic warming through the Fram Strait: Oceanic heat transport from 3 years of measurements, *J. Geophys. Res.*, *109*, C06026, doi:10.1029/2003JC001823.
Schulze, L. M., and R. S. Pickart (2012), Seasonal variation of upwelling in the Alaskan Beaufort Sea: Impact of sea ice cover, *J. Geophys. Res.*, *117*, C06022, doi:10.1029/2012JC007985.
Smedsrud, L. H., R. Ingvaldsen, J. E. Ø. Nilsen, and Ø. Skagseth (2010), Heat in the Barents Sea: Transport, storage, and surface fluxes, *Ocean Sci.*, *6*, 219–234.
Spall, M. A. (1995), Frontogenesis, subduction, and cross-front exchange at upper ocean fronts, *J. Geophys. Res.*, *100*, 2543–2557.
Spall, M. A. (2013), On the circulation of Atlantic Water in the Arctic Ocean, *J. Phys. Oceanogr.*, *43*, 2352–2371, doi:10.1175/JPO-D-13-079.1.
Spall, M. A., R. S. Pickart, P. S. Fratantoni, and A. J. Plueddemann (2008), Western Arctic shelfbreak eddies: Formation and transport, *J. Phys. Oceanogr.*, *38*, 1644–1668, doi:10.10.1175/2007JPO3829.1.
Swift, J. H., E. P. Jones, K. Aagaard, E. C. Carmack, M. Hingston, R. W. Macdonald, F. A. McLaughlin, and R. G. Perkin (1997), Waters of the Makarov and Canada basins, *Deep Sea Res., Part II*, *44*, 1503–1529.
Teigen, S. H., F. Nilsen, and B. Gjevik (2010), Barotropic instability in the West Spitsbergen Current, *J. Geophys. Res.*, *115*, C07016, doi:10.1029/2009JC005996.
Teigen, S. H., F. Nilsen, R. Skogseth, B. Gjevik, and A. Beszczynska-Möller (2011), Baroclinic instability in the West Spitsbergen Current, *J. Geophys. Res.*, *116*, C07012, doi:10.1029/2011JC006974.
Våge, K., R. S. Pickart, M. A. Spall, H. Valdimarsson, S. Jónsson, D. J. Torres, S. Østerhus, and T. Eldevik (2011), Significant role of the North Icelandic Jet in the formation of Denmark Strait Overflow Water, *Nat. Geosci.*, *4*, 723–727, doi:10.1038/NGEO1234.
Våge, K., R. S. Pickart, M. A. Spall, G. W. K. Moore, H. Valdimarsson, D. J. Torres, S. Y. Erofeeva, and J. E. Ø. Nilsen (2013), Revised circulation scheme north of the Denmark Strait, *Deep Sea Res., Part I*, *79*, 20–39, doi:10.1016/j.dsr.2013.05.007.

von Appen, W.-J., and R. S. Pickart (2012), Two configurations of the Western Arctic Shelfbreak Current in summer, *J. Phys. Oceanogr.*, *42*, 329–351, doi:10.1175/JPO-D-11-026.1.

von Appen, W.-J., U. Schauer, T. Hattermann, and A. Beszczynska-Möller (2016), Seasonal cycle of mesoscale instability of the West Spitsbergen Current, *J. Phys. Oceanogr.*, *46*, 1231–1254, doi:10.1175/JPO-D-15-0184.1.

Wernli, H., and C. Schwierz (2006), Surface cyclones in the ERA-40 dataset (1958-2001), part I: Novel identification method and global climatology, *J. Atmos. Sci.*, *63*, 2486–2507.

Woodgate, R. A., K. Aagaard, R. D. Muench, J. Gunn, G. Björk, B. Rudels, A. T. Toach, and U. Schauer (2001), The Arctic Ocean Boundary Current along the Eurasian slope and the adjacent Lomonosov Ridge: Water mass properties, transports, and transformations from moored instruments, *Deep Sea Res.*, *48*, 1757–1792.

Yang, J. (2005), The Arctic and Subarctic ocean flux of potential vorticity and the Arctic Ocean circulation, *J. Phys. Oceanogr.*, *35*, 2387–2407.

Zhao, M., M. L. Timmermans, S. Cole, R. Krishfield, A. Proshutinsky, and J. Toole (2014), Characterizing the eddy field in the Arctic Ocean halocline, *J. Geophys. Res. Oceans*, *119*, 8800–8817, doi:10.1002/2014JC010488.